Defense Technical Information Center
Compilation Part Notice

ADP014134

TITLE: The Role of Spectrum Loading in Damage-Tolerance
Life-Management of Fracture Critical Turbine Engine Components

DISTRIBUTION: Approved for public release, distribution unlimited
Availability: Hard copy only.

This paper is part of the following report:

TITLE: Aging Mechanisms and Control. Symposium Part A -
Developments in Computational Aero- and Hydro-Acoustics. Symposium
Part B - Monitoring and Management of Gas Turbine Fleets for Extended
Life and Reduced Costs [Les mecanismes vieillissants et le controle]
[Symposium Partie A - Developpements dans le domaine de
l'aeroacoustique et l'hydroacoustique numeriques] [Symposium Partie B ...

To order the complete compilation report, use: ADA415749

The component part is provided here to allow users access to individually authored sections
of proceedings, annals, symposia, etc. However, the component should be considered within
the context of the overall compilation report and not as a stand-alone technical report.

The following component part numbers comprise the compilation report:
ADP014092 thru ADP014141

The Role of Spectrum Loading
in Damage-Tolerance Life-Management
of Fracture Critical Turbine Engine Components

James M. Larsen[1], Andrew H. Rosenberger[1], George A. Hartman[2]
Stephan M. Russ[1] and Reji John[1]

[1] Air Force Research Laboratory, Materials and Manufacturing Directorate
AFRL/MLLMN, 2230 Tenth Street, Ste 1
Wright-Patterson Air Force Base, Ohio 45433-7817, U.S.A.

[2] University of Dayton Research Institute
Structural Integrity Division
300 College Park, Dayton, Ohio 45469-0128, U.S.A.

ABSTRACT

Recent developments in experimental and computational capabilities suggest an opportunity to develop improved models of crack growth for use in life management of materials and components in advanced gas turbine engines. Improvements in such models have potential benefits in the sustainment of aging engines, as well as the design of more durable future engines. Current approaches for life management of engine components tend to ignore potential increases in crack propagation lifetime that may occur as the result of load interaction phenomena under variable amplitude spectrum loading. In effort to quantify these potential benefits, a study of updated mission profiles was performed. A variety of engine usage spectra were surveyed to document their cycle content statistically, including characterization of the fundamental load sequence events and the expected severity of damage produced by these events, using data from the advanced nickel-base superalloy IN100.

INTRODUCTION

Current deployment plans by U.S. Air Force dictate that most aircraft be used well beyond their original design lifetimes [1,2]. It has been estimated that replacing the Air Force's existing fleet of aircraft would cost approximately $290B in 1995 dollars [3], while the budget for acquisition of new aircraft is approximately $2-3B per year. Since significant increases in the acquisition budget are unlikely in the foreseeable future, the need for, and cost of, aircraft sustainment will continue to be a major Air Force expense. Moreover, sustainment costs will almost certainly grow substantially over the next few years, as the large number of aircraft acquired in the 1980's continue to age. The National Materials Advisory Board (NMAB) report on Aging of U.S Air Force Aircraft [2] clearly defined this problem and identified technology needs to support sustainment of aircraft structures. To make the NMAB study tractable, the issue of aging turbine engines was excluded from consideration, although the board's chairman, C. F. Tiffany, noted that aging engines were a major concern and should be the subject of a future study.

Aging turbine engines are traditionally viewed as being more easily maintained than aging aircraft, since engines are disassembled during periodic overhauls, making replacement of aging engine components a comparably straightforward process. However, the current cost of engine maintenance represents over 60% of the Air Force's annual budget for turbine engines. This budget also includes

engine development, acquisition, and about 2.6% for science and technology. A key aspect of the engine maintenance process is the life management of fracture critical components, such as engine disks and spacers, as specified by the Engine Structural Integrity Program (ENSIP) [4]. Such components are most critical in single-engine fighter aircraft, since component failure normally results in loss of the aircraft. The cyclic safe-life of such components is typically defined as the point at which the probability of initiating a 0.79-mm surface crack is predicted to be 1/1000. In addition, to preclude effects of possible rogue flaws, the crack propagation lifetime from a possible initial material defect must equal or exceed the design life. When the component service life reaches the design life, the component is to be replaced. Unfortunately, the 0.79-mm crack-initiation requirement necessitates that 99.9% of the components be retired prematurely in order to assure removal of the remaining 0.1% of components that are predicted to contain such a crack. Although this life-management approach has been effective in assuring flight safety, evidence suggests that it may be highly conservative in many instances. This conservatism contributes to high maintenance costs and may limit readiness, if the necessary spare parts are unavailable.

An alternative approach, known as inspection-based life management or retirement for cause, relies on nondestructive evaluation (NDE) to identify crack-like damage, which is then used as the primary basis for component retirement. To assure safety, the minimum remaining crack propagation lifetime should be at least twice the inspection interval. Typical fighter aircraft engines are designed for a nominal life limit of 8000 total accumulated cycles (TACs), which equates to a lifetime of approximately 10 to 14 years at current rates of aircraft usage. These engines undergo an overhaul and safety inspection at their half-life.

Many of the engines in the Air Force's fleet of F15 and F16 aircraft will soon reach their design lifetimes, which is expected to result in a major wave of increased engine sustainment costs as the aging components are replaced. However, it has been estimated [5] that extending the operational life of 60% of the disks in F16 and F15 aircraft by one inspection interval, nominally from 8000 to 12000 TACs, would result in a cost avoidance on the order of $600M over the period of 2005-2010, and substantially more in the long run. Such a life extension might be expected to produce an accompanying increase in the risk of catastrophic failure. However, current projections indicate that it should be possible to extend the lives of many components in today's engines without increasing overall risk, if key improvements in life management technology are developed and implemented. Many of these technologies would also apply to life management of future engines, which could be designed to optimize durability and affordability.

To address these issues, the U.S. Air Force is embarking on a technology development and implementation initiative, known as the Engine Rotor Life Extension (ERLE) program, which is organized to reduce the cost of sustainment of its current fleet of advanced turbine engines. The ERLE program, which is part the larger Versatile Affordable Advanced Turbine Engine (VAATE) program [6] and its National Turbine Engine Durability initiative, has the goal of extending the useful lifetime of major, fracture-critical components in currently fielded gas turbine engines, while maintaining or improving overall engine safety and reliability. Full achievement of the ERLE objectives will require improvements in a broad range of technologies, including nondestructive evaluation, engine usage and health monitoring, life prediction and fracture mechanics, data fusion, and component repair. The current paper highlights some of the background and opportunities for improvement in the area of life prediction and life management based on fatigue crack growth, with a specific focus on effects of engine operating spectra on fatigue crack growth under cycle- and time-dependent conditions.

ENGINE MISSION LOADING

It is well known that loading spectra of major rotating components in engines typically exhibit less variability than spectra experienced by aircraft structures [7,8,9]. The major cycles in mission spectra for these rotating components result from variations in engine speed produced by throttle excursions for take-off, in-flight maneuvers, and landing. For components exposed to elevated temperatures there is additional stress imposed by thermal gradients and thermal transients produced by variations is operating conditions and heat transfer within the engine. A schematic of a flight profile showing the simplified elements of a typical flight is illustrated in Fig. 1 [7]. This figure shows normalized spectra for routine engine operating speeds and associated temperatures for a given location on a generic component. As shown, the maximum loading tends to occur at takeoff, although additional, but infrequent, full-power excursions may occasionally reach this maximum level. Hold periods of constant stress occur at moderate stress (60 to 65% of maximum) representative of cruise or transit portions of the mission. Major rotating components, such as disks and spacers, are typically designed such that their maximum stresses at full power are only slightly below the component burst stress at the operation temperature.

The engine-component design practices, combined with the relatively controlled nature of the mission spectra, tend to obviate the large effects of load sequence, or load interaction, on crack growth that are often common in fatigue spectra of airframe structures. Depending on the nature of the load sequence, such load interaction effects can produce either crack acceleration or crack retardation [10], although the latter is far more common. Crack retardation tends to occur in fatigue cycles that follow an overload, and this effect can be extremely significant, particularly as the overload ratio (OLR) increases. Here we define the OLR to be σ_{max} of the overload divided by σ_{max} of the subsequent cycles. Airframe spectra may contain cycles with OLRs well in excess of 2 or 3, while experience with engine spectra has suggested that a limiting OLR of 1.25 is common. Such conclusions were drawn by a NATO AGARD task group established in the early 1980s to develop a loading standard for fighter aircraft engine disk usage [11]. This task group developed TURBISTAN, a test spectrum applicable for titanium alloys operating at or near ambient temperature. Noteworthy from analysis of the TURBISTAN load spectrum was that the spectrum tended to approximate a simple sequence containing a high stress ratio baseline with periodic underloads, where the underloads in this case were at loads near zero – but not compressive.

Typical Loading Spectra for Major Rotating Components

Data on engine usage profiles are continually collected and used to update the life analyses. Figures 2a and 2b present recently obtained examples of loading and temperature histories for a specific location on a titanium-alloy rotor component during a single flight. These spectra correspond to a single ground-air-ground cycle and indicate the low-cycle-fatigue (LCF) nature of the loading and the extent of stress and temperature variability for this modest-temperature component location. Figure 2c plots the relationship between stress ratio ($R = \sigma_{min}/\sigma_{max}$) and normalized maximum stress for each of the individual loading cycles depicted in Fig. 2a. The data indicate that almost all of the cyclic loading occurs under a relatively high stress ratio, combined with a correspondingly high normalized stress. These loading conditions are the result of the combined effects of changes in engine speed, coupled with the effects of thermally induced stresses. The relationship between stress and temperature is illustrated in Fig. 2d, where normalized stress is plotted versus temperature for each reversal point in the stress spectrum. This figure also shows that stress and temperature are negatively correlated, that is, stress and temperature tend to be out-of-phase for the majority of the fatigue cycles. The loading may be further quantified by plotting a histogram of the normalized stress, as illustrated in Fig. 2e, which shows that a majority of the cycles have maximum stress levels greater than 70% of the maximum mission stress. Alternatively, one can calculate the ratio of the maximum cyclic stress to the maximum mission stress - the OLR. Defining the maximum stress in Fig 2a as an overload, the OLR of the remaining cycles was calculated, and a histogram of the results in plotted in Fig 2e. This figure shows that many of the cycles experience OLRs in the range of 1.25, consistent with the earlier reports. Notably absent in the spectrum is any significant hold time near a constant load of appreciable magnitude.

A second stress spectrum for a higher-temperature, nickel-base-superalloy component is show in Fig. 3a, and the corresponding temperature spectrum is shown in Fig. 3b. In this case the fatigue stress cycles have a larger relative amplitude, and a significant compression cycle occurs when the engine is powered down and cools slowly to ambient temperature. The relationship between stress ratio and temperature is plotted in Fig. 2c, and a stress versus temperature plot is presented in Fig. 3d. As shown in the latter figure, this mission and component location also exhibits an out-of-phase stress-temperature relationship for most fatigue cycles. Figures 3d and 3e, respectively, show histograms of the cyclic maximum load data and the corresponding OLRs. The majority of the maximum loads in cycles with high values of maximum load are centered on a value of approximately 0.7 times the maximum mission load. As shown in Fig. 3e, in terms of overload ratio, this corresponds to values of OLR approximately centered about a value of 1.4, with a substantial number of cycles above this level. This trend is in contrast to the data of Fig. 2e from the lower-temperature titanium-alloy component, wherein the OLRs more commonly fell around 1.25. Like the earlier spectrum, the spectrum in Fig. 3 does not exhibit significant periods of sustained loading.

HIGH-TEMPERATURE LOAD SEQUENCE EFFECTS IN IN100

The powder metallurgy, nickel-base alloy IN100 was chosen as a representative material for assessment of the role of turbine engine load sequence effects on crack growth. This material was selected for several reasons: (1) as noted above, the more extreme mission stress spectrum was observed in the higher-temperature, nickel-base-alloy component, (2) IN100 is in widespread use in advanced engines, (3) a substantial database for this alloy was already available, and (4) this material is representative of other high performance, powder-metallurgy, nickel-base alloys used throughout the turbine engine industry. The specific material chosen was superplastically forged and heat treated by Pratt & Whitney according to their alloy specification PWA 1073. This produced the fine uniform microstructure of primary gamma-prime grains in gamma-gamma prime matrix shown in Fig. 4.

A U.S. Air Force contract report by Pratt & Whitney served as the primary reference for data on this material [7]. This report demonstrated that the main parameters controlling high-temperature fatigue crack growth in this alloy were temperature, frequency, and stress ratio. These data were obtained from tests of compact tension, C(T), specimens in accordance with ASTM standard E-647. For most cases, the range in ΔK over which the tests were performed was limited by the relatively low fatigue frequencies used and the resulting long test times.

Figure 5 plots the effect of temperature on fatigue crack growth for temperatures ranging from 538 to 732 °C, at a frequency of 0.167 Hz, or 10 cycles/minute. For the data shown, the crack growth rate increased by a factor of approximately 3 to 4 as the temperature increased from 538 to 732 °C. The curves shown in the figure and the subsequent plots represent the correlation provided by an interpolative hyperbolic-sine regression model originally developed by Annis et al [12,13,14]. This model provides a mathematical representation of effects of temperature, frequency, stress ratio, and load-sequence effects.

Figure 6 shows crack growth data for tests of IN100 at a temperature of 649 °C as a function of frequency, ranging from 0.00833 to 20 Hz. Over this range in increasing frequency, the crack growth rate decreased by a factor of approximately 5 to 7, depending on the applied ΔK. Figure 7 shows data collected at 649 °C, a frequency of 0.167 Hz, and stress ratios ranging from 0.1 to 0.8. For a given value of ΔK, this range in stress ratio resulted in an increase in crack growth rate by a factor of approximately 3 with increasing R.

When considering effects of variable-amplitude loading, it is convenient to define loading parameters in terms of the stress ratio of the baseline fatigue cycle, the OLR, and the number of baseline cycles between overloads (CBO). These parameters are depicted schematically in Fig. 8, which shows

blocks of constant-load-amplitude fatigue interrupted by periodic overloads. By testing under repeated blocks of such cycles, one can quantify the effects of load interactions that simulate the key elements comprising a typical engine mission. Figure 9 shows effects of applying one cycle at an OLR of 1.5, followed by 40 cycles of baseline fatigue loading at an R of 0.5. As shown, increasing from no overload (OLR = 1.0) to a relatively modest overload (OLR = 1.5) results in a reduction in the crack growth rate of approximately a factor of 4 due to the action of the overload. This effect is further revealed in Fig. 10, which shows the effect of increasing the number of CBO from 5 to 40 with an OLR of 1.5. As shown, this increase in the number of CBO produced a reduction in crack growth rate by a factor of 5 or more. This effect was particularly accentuated at lower values of ΔK.

To extend the understanding of load-sequence effects in IN100, a focused study of crack growth rates was conducted under repeated mission-element cycle blocks of the type shown in Fig. 8. In this study, spectra were applied under constant-K-controlled conditions, rather than constant-load-controlled conditions. This specialized testing method incorporates a greatly improved direct-current potential-difference technique for measurement of crack length. This improved technique results in substantial improvements in the accuracy and precision of corresponding calculations of da/dN, and the time required to perform key experiments is greatly reduced. Tests were performed on C(T) specimens using repetitive fatigue blocks composed of a single overload followed by a block of constant-ΔK cycles. In each case the crack was extended until it became clear that a macroscopic steady state crack growth rate had been achieved, which was indicated by a linear crack-length vs. cycles (a vs. N) response. In this manner any transient behavior due to changes in the type of spectrum being applied was clearly identified and excluded from the valid data.

These tests were performed under a variety of loading conditions, which are exemplified by the data presented in the lower region of Fig. 11. This graph plots crack growth rate as a function of the number of CBO for OLRs of 1.125, 1.25, 1.375, and 1.5, and the experimental results are indicated by solid symbols and connected by dotted lines. The tests were performed in air at 649 °C, a frequency of 0.167 Hz, R = 0.5, and K_{max} of the baseline cycles = 30 MPa$\sqrt{m}$. The horizontal line represents the crack growth rate observed under this baseline constant-K-amplitude condition. The upper region of this plot also shows calculations of crack growth rate obtained by a linear summation of the contribution from one overload cycle plus the given number of CBO, ignoring any possible load interaction effects. This simple approximation shows that the expected growth rate approaches the baseline value as CBO increases.

In contrast to the simple approximation, the data for the overload tests show that the crack growth rate quickly drops below the baseline growth rate as CBO increases. When CBO is zero, the crack growth rate corresponds to constant amplitude cycling under the overload condition. As CBO is increased, the resulting average crack growth rate soon drops below the baseline rate. At a CBO of 40, the growth rates for the higher OLR experiments fell substantially below the baseline. To further examine the influence of OLR, a number of additional experiments were performed as a function of OLR with CBO held constant at 40, Fig. 12. This figure shows a continually reducing growth rate as OLR was increased from 1.0 (no overload) to 1.6. As shown, relatively minor overloads produced a reduction in crack growth rate, and the greatest reduction in crack growth rate occurred in the approximate range of 1.0 < OLR < 1.3.

To further reveal the behavior of the observed load-interaction effect, the procedure depicted in Fig. 13 was performed, wherein the results for a given OLR were used to deduce the instantaneous crack growth rate following an overload. Under this procedure, the local crack growth rate following an overload is deduced by subtracting effects of successive cycle blocks. For example, subtracting the crack growth during a 20-CBO block from the growth observed during a 40-CBO block gives the apparent average growth rate contribution from cycles 21 through 40, which eliminated the apparent effect of the initial portion of the block, including the overload. By performing this procedure on successively smaller blocks, the data shown in Fig. 14 were obtained. These data indicate that the local crack growth rate

following an overload is reduced almost immediately, and that continued crack growth retardation is almost constant until the subsequent overload interrupts and restarts the process. For example, the apparent growth rate for an OLR of 1.5 drops after one cycle to a value that is approximately an order of magnitude below the baseline rate.

SUMMARY AND CONCLUSIONS

To address the growing financial and logistical costs of sustainment of turbine engines, the U. S. Air Force is investing in a range of science and technology initiatives to improve and extend capabilities for component life management. Recent advances in computational and experimental capabilities present important opportunities for development of more accurate and robust life-management technologies. In support of models of damage tolerance and fatigue crack growth, the current study surveyed a number of updated turbine-engine mission-usage histories. From these data it appears that the combination of loading and thermal histories may produce appreciable variations in stress, particularly in some of the higher temperature components that experience significant thermally induced stresses. As produced by variations in engine speed, the majority of the engine duty cycles occur at relatively high stresses, presenting the opportunity for load sequence effects.

The potential magnitudes of the effects of key mission usage variables were assessed using data from the superalloy IN100 from the literature, plus data generated using a newly developed constant-K-controlled experimental capability. This method, which also used a much improved direct current potential difference technique for measurement of crack length, provided a unique capability to perform highly specialized load-sequence experiments quickly. It was shown that the role of mission load sequence events can produce variations in crack growth rate that are as significant as those produced by the more common primary variables of temperature, frequency, and stress ratio. In tests of simplified mission elements containing relatively modest overloads, reductions of crack growth rate of a factor of four were observed, and the greatest sensitivity in crack-retardation occurred over the interval of overload ratios from 1.05 to 1.3. These findings suggest that a potentially significant beneficial effect of load sequences may be expected under typical mission loading.

ACKNOWLEDGEMENTS
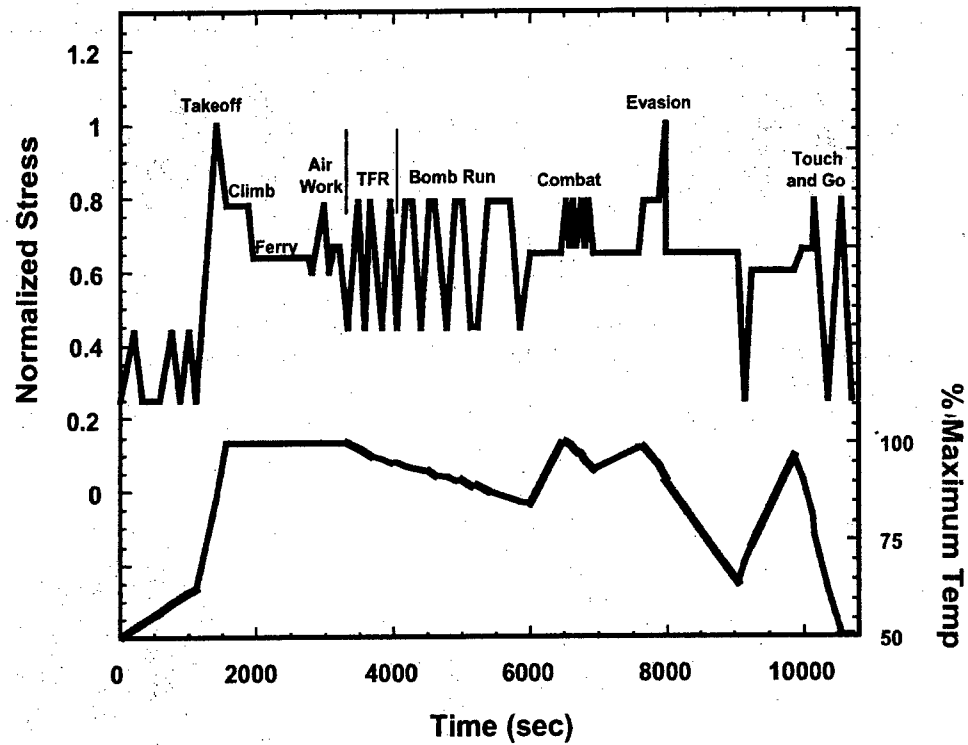
Figure 1. Schematic of typical mission loading and temperature spectra for high temperature military turbine engine rotor components, such as disks.
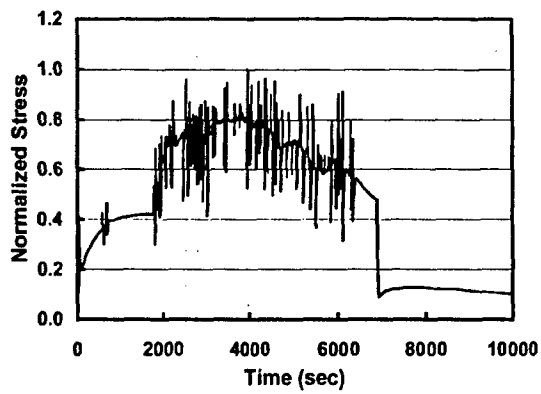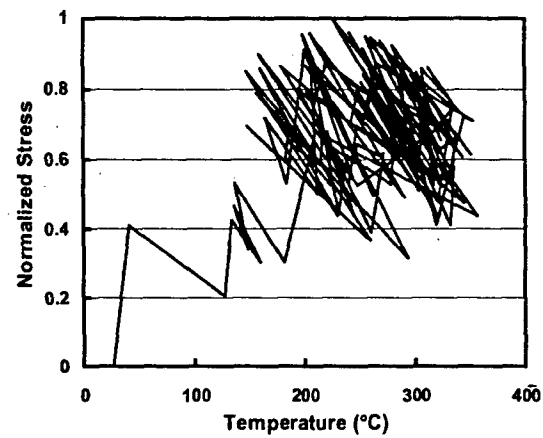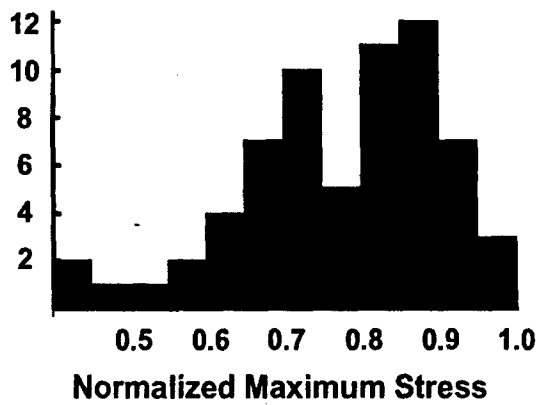
(a) Stress-time mission history
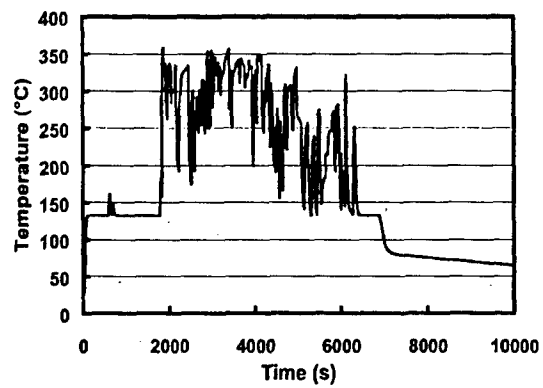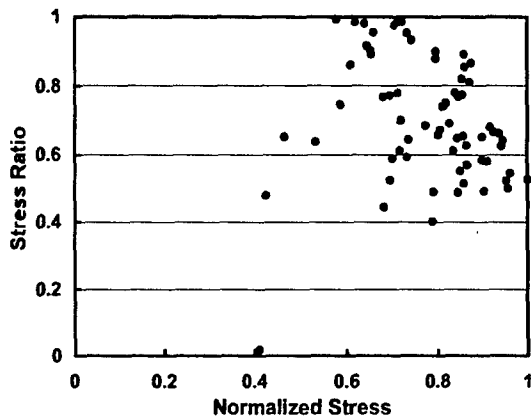
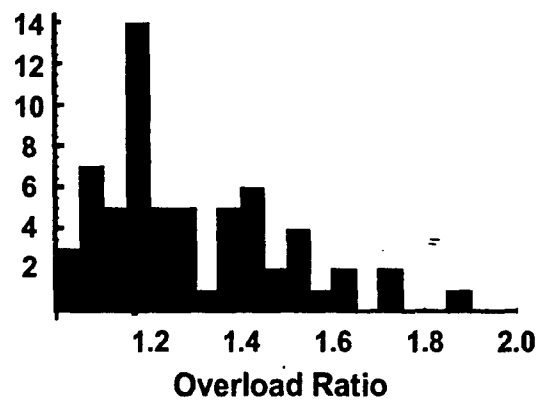(b) Temperature-time mission history

(c) Stress ratio vs. normalized stress
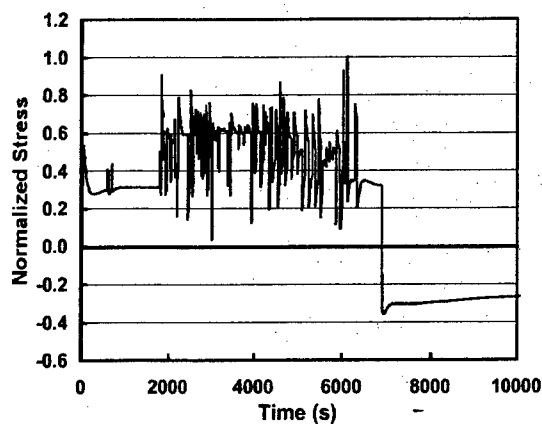
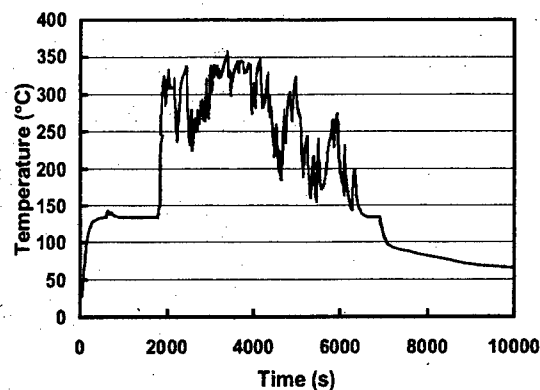(d) Stress-temperature mission history

(e) Histogram of maximum stresses

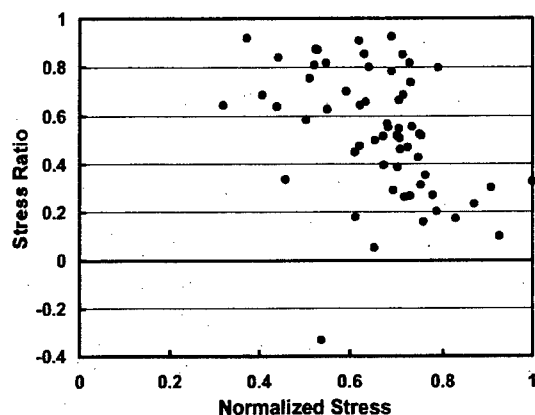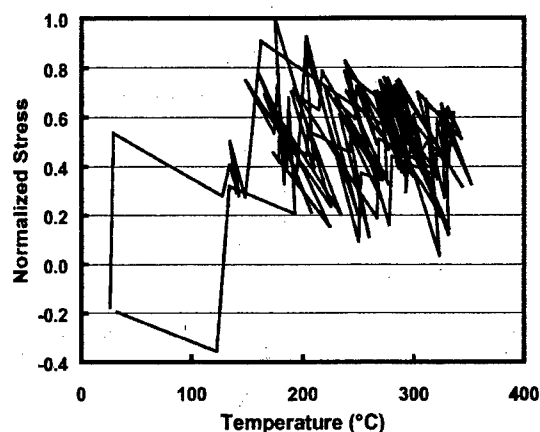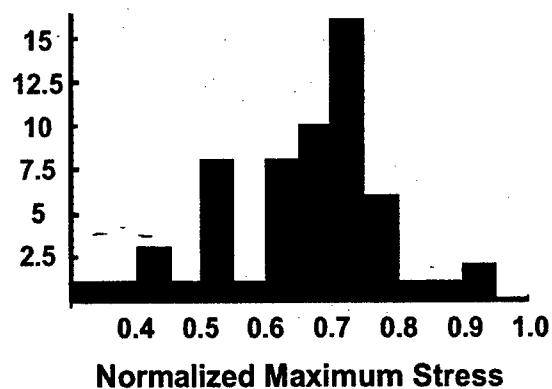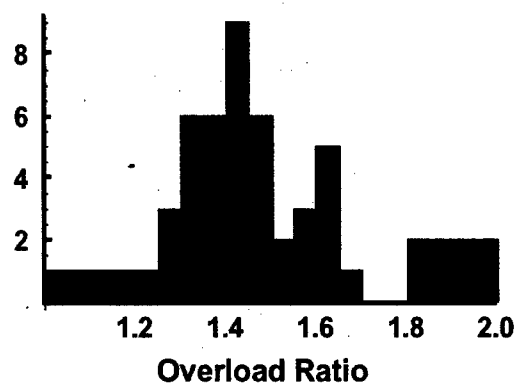(f) Histogram of overload ratios (OLRs)

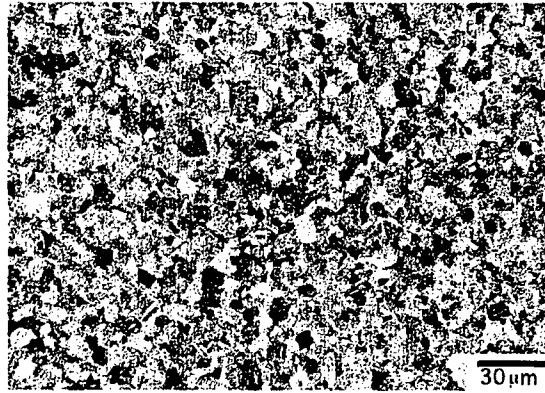Figure 2. Typical engine mission data for a titanium alloy component.

(a) Stress-time mission history

(b) Temperature-time mission history

(c) Stress ratio vs. normalized stress

(d) Stress-temperature mission history

(e) Histogram of maximum stresses

(f) Histogram of overload ratios

Figure 3. Typical engine mission data for a nickel-base superalloy component.

Figure 4. Microstructure of IN100
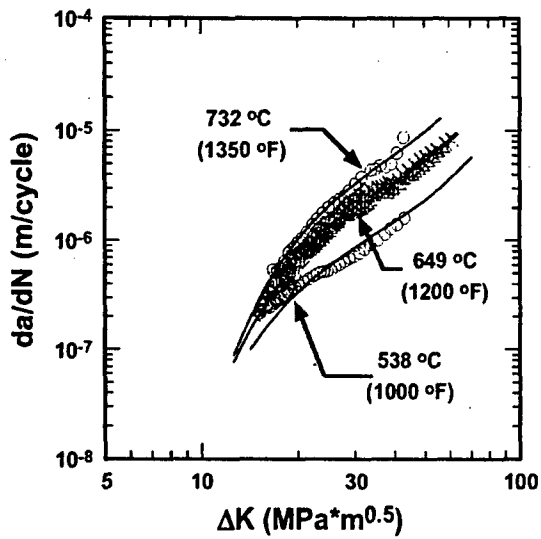
Figure 5. Effect of temperature on crack growth in IN100; R = 0.1, Freq. = 0.167 Hz.
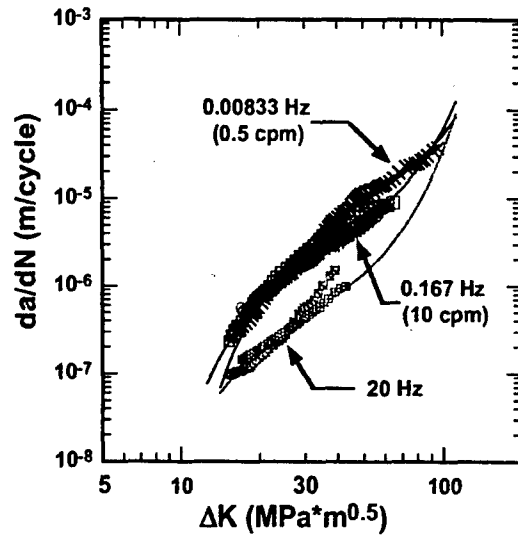
Figure 6. Effect of frequency on crack growth in IN100; T = 649°C, R = 0.1.
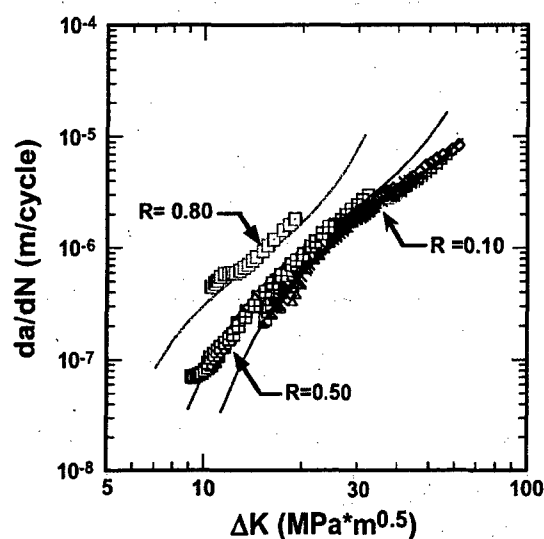
Figure 7. Effect of stress ratio on crack growth in IN100; T = 649°C; Freq. = 0.167 Hz.
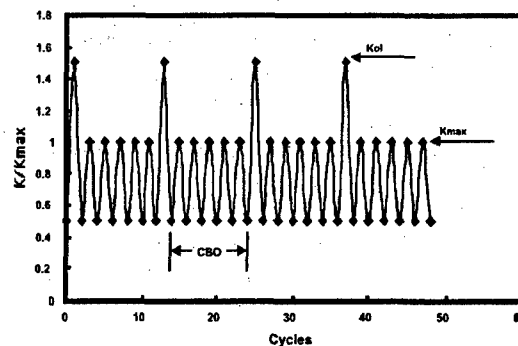
Figure 8. Schematic of simplified mission element containing repeated overloads and a fixed number of cycles between overloads (CBO).
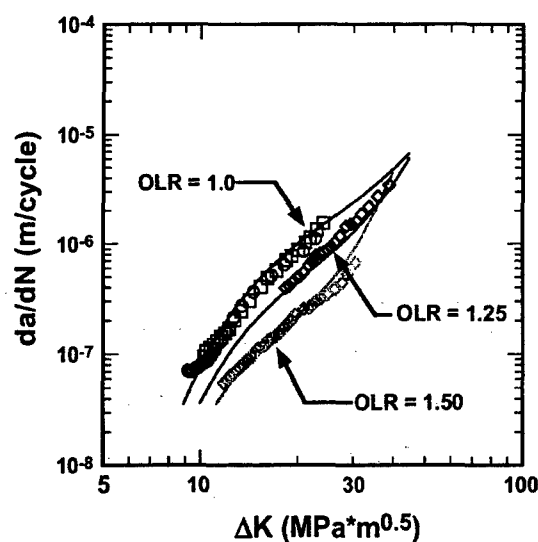

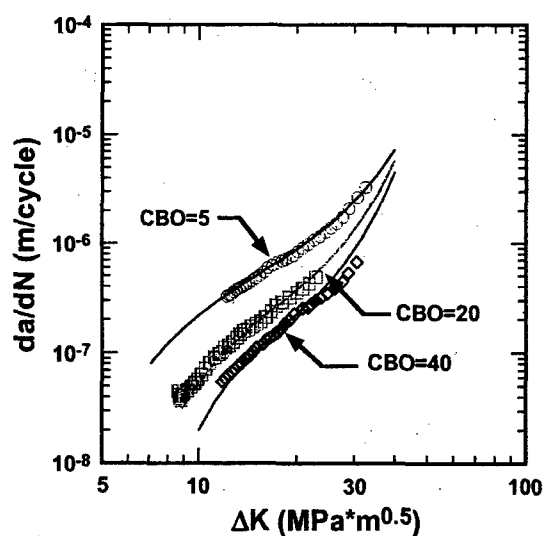Figure 9. Effect of overload ratio (OLR) on crack growth in IN100; T = 649°C; R = 0.5, Freq. = 0.167 Hz, CBO = 40.

Figure 10. Effect of number of cycles between overloads (CBO) on crack growth in IN100; T = 649°C; R = 0.5, Freq. = 0.167 Hz, OLR = 1.5.
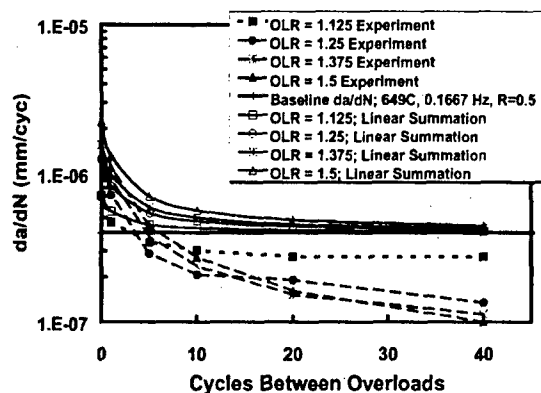
Figure 11. Crack growth behavior plotted as a function of the number of cycles between overloads (CBO) for K-controlled block loading illustrated in Fig. 8. T=649°C, Frequency = 0.167 Hz, R = 0.5, K_{max} = 30 MPa*m$^{0.5}$. Also shown are the baseline growth rate under the same conditions and the growth rates predicted by a linear summation technique.
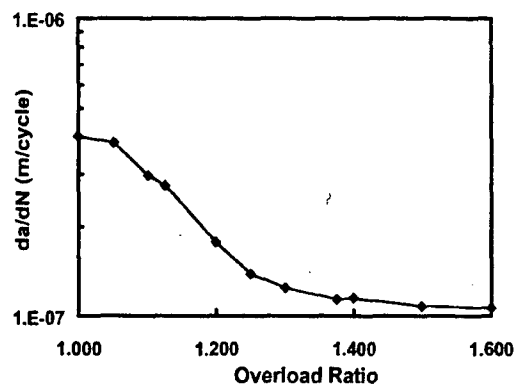
Figure 12. Crack growth behavior plotted as a function of the overload ratio with CBO = 40. T=649°C, Frequency = 0.167 Hz, R = 0.5, K_{max} = 30 MPa*m$^{0.5}$.
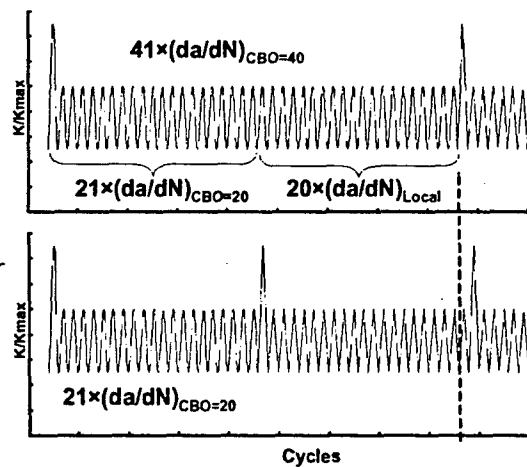

Figure 13. Schematic illustrating how the local crack growth in the baseline cycling following an overload block is determined.
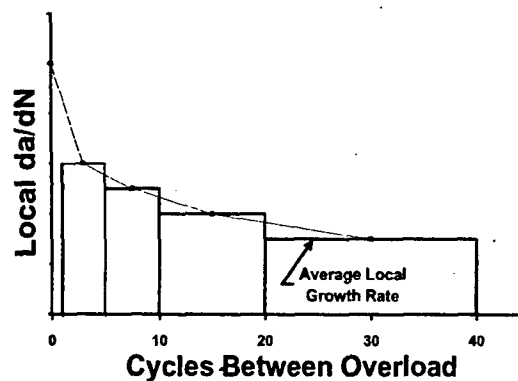
Figure 14. Schematic of the average local crack growth rate in the baseline cycling following an overload block.
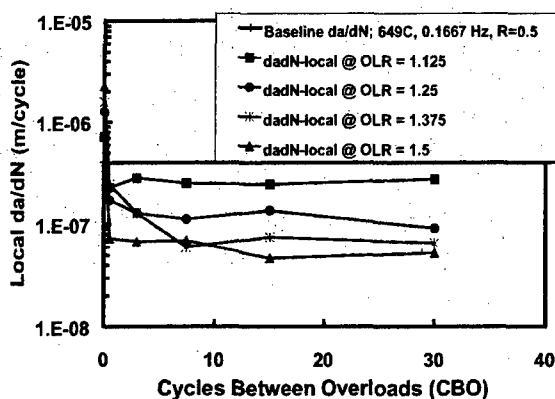
Figure 15. Local crack growth in the baseline cycles following an overload block behavior plotted as a function of the average number of cycles between overload following the schema in Figs 13 and 14. T=649°C, Frequency = 0.167 Hz, $R = 0.5$, $K_{max} = 30$ MPa*m$^{0.5}$.

REFERENCES

1. SAB (Scientific Advisory Board), Report of the Ad Hoc Committee on Life Extension and Mission Enhancement for Air Force Aircraft, U.S Air Force Scientific Advisory Board, Washington, D. C., Department of the Air Force, Report TR-94-01, 1994.
2. NMAB (National Materials Advisory Board), Aging of U.S. Air Force Aircraft, National Research Council, National Academy Press, Washington, D.C., Publication NMAB-488-2, 1997.
3. Hadcock, R. N., "Aging Airframe Structural Life Enhancement: An Overview," presented at The First Joint DOD/FAA/NASA Conference on Aging Aircraft, Ogden, Utah, July, 1997.
4. U.S. Air Force, Engine Structural Integrity Program, Military Standard 1783, Aeronautical Systems Division, Wright-Patterson Air Force Base, OH, 1984.
5. Reimann, W. H., "U.S. Air Force Turbine Engine Maintenance Practices", Air Force subcontract report, 1997.
6. Stricker, J., "Advanced Turbine Engines – A Strategic Vision", presented at the World Aviation Conference, San Diego CA, Nov., 1999.
7. J. M. Larsen, B. J. Schwartz, and C. G. Annis, Jr., "Cumulative Damage Fracture Mechanics Under Engine Spectra," Air Force Materials Laboratory Report AFML-TR-79-4159, Wright-Patterson AFB, OH, 1979.
8 Larsen, J. M. and Nicholas, T., "Cumulative Damage Modeling of Fatigue Crack Growth," AGARD Conference Proceedings No. 368, Engine Cyclic Durability by Analysis and Testing, Advisory Group for Aerospace Research and Development, Neuilly sur Seine, France, 1984, pp. 9-1 – 9-15.
9 Larsen, J. M. and Nicholas, T., "Cumulative-Damage Modeling of Fatigue Crack Growth in Turbine Engine Materials," Engineering Fracture Mechanics, Vol. 22, No. 4, 1985, pp. 713-730.
10. Russ, S. M., Rosenberger, A. H., Larsen, J. M., and Johnson, W. S., "Fatigue Crack Growth Predictions for Simplified Spectrum Loading: Influence of Major Cycles on Minor-Cycle Damage Rates," in this proceedings, 2001.
11 Mom, A. J. A, Evans, W. J., and ten Have, A. A., "TURBISTAN, a Standard Load Sequence for Aircraft Engine Discs," AGARD Conference Proceedings No. 393, Damage Tolerant Concepts for Critical Engine Components, Advisory Group for Aerospace Research and Development, Neuilly sur Seine, France, 1985, pp. 20-1 - 20-11.

12. C. G. Annis, Jr., R. M. Wallace, and D. L. Sims, "An Interpolative Model for Elevated Temperature Fatigue Crack Propagation," Air Force Materials Laboratory Report AFML-TR-76-176, Part I, Wright-Patterson Air Force Base, OH, 1976.
13. R. M. Wallace, C. G. Annis, Jr., and D. L. Sims, "Application of Fracture Mechanics at Elevated Temperature," Air Force Materials Laboratory Report AFML-TR-76-176, Part II, Wright-Patterson Air Force Base, OH, 1976.
14. D. L. Sims, C. G. Annis, Jr., and R. M. Wallace, "Cumulative Damage Fracture Mechanics at Elevated Temperature," Air Force Materials Laboratory Report AFML-TR-76-176, Part III, Wright-Patterson AFB, OH, 1976.